A Delay-based Neuromorphic Processor for Arrhythmias Detection

***Abstract*— Cardiovascular disease is the leading cause of global mortality, with 17.5 Million deaths per annum (World Health Authority, WHO). Innovative hardware based cardiac recording devices could help elevate this burden. Delay-based reservoir computing is a novel computational framework with only a single nonlinear node. This feature makes it a strong candidate for the hardware implementation of an analogue cognitive system. Such a system can be exploited to improve the energy efficiency of data processing in implantable bioelectronic devices. This paper presents a system modelling of this network that is capable of cognitively processing Electrocardiograph (ECG) signals from the MIT-BIH arrhythmia database. The proposed single-input single-output model receives an encoded ECG signal while the output amplitude pattern aids the diagnostic interpretation. The information processor is an analogue circuit with the dynamic properties of Mackey-Glass nonlinearity and fading memory. To validate this system and mimic real-time operation, the simulation is designed to detect ventricular ectopic beats, an ectopic heartbeat type, using a continuous ECG signal without any signal segmentation or feature extraction. After training, the model successfully locates ventricular ectopic beat with 87.51% sensitivity and 94.12% accuracy for the testing dataset from three patients.**

Keywords—Delay-based reservoir computing; Arrhythmias Detection; Neuromorphic processor; Pattern recognition; Analogue cognitive system.

I. INTRODUCTION

Within the next decade Moore's law, which dictates the exponential growth in chip transistor density, will inevitably reach its limit due to fundamental material and physical constraints of computing architecture [1-3]. To further boost the computational capability, one of the solutions involves investigating novel architectures. The artificial neural network, as a brain-inspired framework, would be much faster and more power-efficient under a neuromorphic architecture rather than current binary systems. For the machine learning tasks, a neuromorphic processor with an analogue computing unit would be a strong alternative of conventional Von Neumann architecture [3-6].

Inspired by the interconnection of brain's neurons and synapses, artificial neural networks are a simplified computational model of biological neural networks used for performing machine learning tasks like pattern recognition and prediction [2, 4, 7]. Delay-based reservoir computing (DRC) is a recently introduced cognitive framework for implementing an artificial neural network

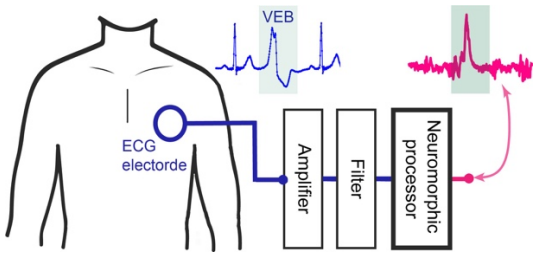

Fig. 1. The conceptual picture of arrhythmia detection using neuromorphic processor.

by using one artificial neuron. It fundamentally can be classified as Recurrent Neural Network (RNN) which links the current input to the past network states. The main difference between the classical RNN, for example reservoir computing, and DRC is that the DRC's reservoir consists of only one artificial neuron and a delay line. The delay line creates a series of virtual nodes for complex reservoir dynamics. These interesting features make DRC a promising candidate of a physical neural network. The physical reservoir computing can significantly improve the efficiency of data processing compared with software-based reservoir computing [4, 8-10].

Since DRC was first proposed [8], it has gradually become the centre of attention and was experimentally evaluated using an optical system [10], electrical systems [9] and even spintronic systems [11]. In this paper, we proposed a modelling of electrical DRC system under MATLAB and Simulink. Two important features of DRC, nonlinearity and fading memory, were achieved by a Mackey-Glass typed analogue circuit and a digital delay line respectively for creating a nonlinear and recurrent connection of each input.

Our aim in this paper is to provide a model that analyses the behaviour of hardware-based DRC for the future development of low power wearable arrhythmia detectors as shown in Fig. 1. Furthermore, we first applied DRC to a continuous arrhythmia detection task without widely-used ECG signal processing procedures like QRS detection, segmentation and feature extraction.

The data was obtained from the MIT-BIH arrhythmia database[12], which was comprehensively analysed and processed using advanced algorithms such as Echo State Network and cycle Echo State Network [13, 14]. The Echo State Network can be considered as a fundamental of DRC [4]. However, most of the state-of-the-art ECG classifications rely on segmentation and feature extraction that are not desired in a low-power neuromorphic device [4,

13-15]. Compared to the other algorithms, DRC based neuromorphic hardware consumes less power, especially in nonlinear processing unit. We directly inject the raw data of the ECG leads (upper signal (MLII) as a continuous signal. We found that high feedback strength results in a reservoir state for more previous input samples. This operation fully utilizes the recurrent feedback to map the whole ECG spectrum onto the network dynamic of DRC. With the specific system design for ECG signal processing, the model is capable of correctly locating 87.51% of the Ventricular Ectopic Beat (VEB) type of ectopic heartbeat for three selected datasets with a number of multiform VEB, which will be explained in detailed.

This paper is organized as follow: Section II introduced the overall system design and the modelling in Simulink. The principal of ECG signal processing including pre-processing, post-processing and system dynamic is provided in Section III. The experimental result and conclusion are presented in Section IV and Section V respectively.

II. Network Description and Reservoir Modelling

A. Principal of DRC

Reservoir computing was first proposed in [16] and [17] independently as an efficient implementation of RNN since only the synapsis connection between reservoir and output layer need to be trained. Inherited from RNN, reservoir computing is particularly good at processing time-dependent data or time-series signal like ECG in real-time because of the effect of past network states existed in each current input. As illustrated in Fig. 2(a), the reservoir architecture consists of an input layer, output layer and a reservoir. There are three groups of weighted connections that need to be defined between layers: the random input ($W_{in}^{res} \in \mathbb{R}^{N\times d}$), random reservoir ($W_{res}^{res} \in \mathbb{R}^{N\times N}$) and trained output ($W_{res}^{out} \in \mathbb{R}^{l\times N}$), where *d, l* and *N* denote input dimension, output dimension and reservoir size, respectively. Only W_{res}^{out} needs to be trained by using labelled data while W_{res}^{res} and W_{in}^{res} are randomly generated [14, 16, 18]. According to the MIT-BIH database [12], the input is designed as a two-dimensional matrix from the two ECG leads. After receiving the input projection, the complex dynamic of reservoir maps the input onto a high- or even infinite-dimensional space where the multi-dimensional input data is more separable. At *n* time step, the reservoir dynamic is governed by:

$$x(n) = f[\beta W_{res}^{res} x(n-1) + \gamma W_{in}^{res} u(n)] \qquad (1)$$

where *x(n)* is an *N*-dimensional vector representing the reservoir states, *f* is an activation function, β and γ are the input and recurrent feedback scaling parameters respectively and normally we set $\beta+\gamma=1$. A larger β/γ ratio results in a longer fading memory. This feature is essential for our raw ECG data input since the fading memory contains the entire heartbeat information after this heartbeat is sent to the network.

After injecting a dataset with length *l* to *u(n)*, we can collect a $k\times N$ matrix of node states *X*. For the training dataset, we will have the desired output or label *y*. The W_{res}^{out} is obtained by minimizing the error $||W_{res}^{out} X - y||^2$, where *y* is the expected output or label of the training input *u(n)*. The ridge regression is applied to get the W_{res}^{out}:

$$W_{res}^{out} = (X^T X + \lambda I)^{-1} \cdot X^T y \qquad (2)$$

where λ is a regularization coefficient to avoid overfitting and *I* denotes the identity matrix. During the testing, the same procedure and dynamic system are applied to the testing dataset. By receiving each node state $X_{test}(n) \in \mathbb{R}^{l\times N}$, the output can be calculated:

$$y(n) = \sum_{i=1}^{N} W_{res}^{out}{}_i \cdot X_{test}(n)_i \qquad (3)$$

After tremendous successes of RC in processing empirical data such as chaotic time series and speech data [3], other research in 2011 introduced a delay line to replace the randomly generated reservoir connection [8], which dramatically reduced the components required to form a

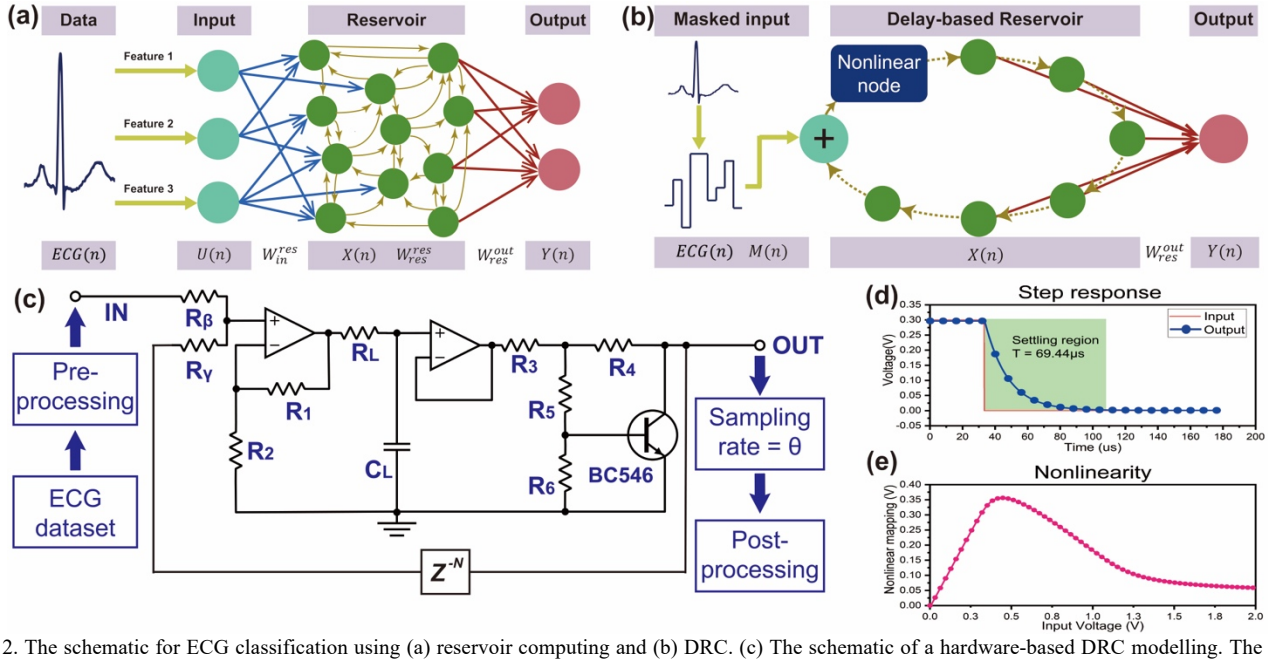

Fig. 2. The schematic for ECG classification using (a) reservoir computing and (b) DRC. (c) The schematic of a hardware-based DRC modelling. The blue blocks are defined by MATLAB while Simulink carries the black part. The circuit is a neuromorphic processor that consists of a non-inverting summing amplifier, nonlinear node and delayed feedback. (d) The step response and (e) nonlinearity of the nonlinear node. The curves are taken by the following parameters: R_L = 3500Ω, C_L= 4nF, R_3 =1kΩ, R_4 =500Ω, R_5 =1kΩ, R_6 =200kΩ.

hardware-based reservoir. As shown in Fig. 2(b), the delay line, with total time τ, is equally divided into (N-1) section to establish N virtual nodes. The separation of each two neighbouring nodes is θ, which results $\tau = N \times \theta$. After the flow in delay line, the output of the nonlinear node will be weighted and summed with the input to create recurrent connection.

The actual operation is a sampling rate of θ applied to the nonlinear node while the output is kept in a delay buffer with a length of τ and then combined with the input. For time-series data input, τ should be equal to the input sampling rate. Another important setup is the settling time of nonlinear node T. By keeping $\theta<T<\tau$, the state of each virtual node will link to the state of previous nodes, which hugely improve the dynamic complexity and performance [8, 9]. In our modelling we choose the empirical setting of T and N: $T = 5 \times \theta$ and $VN = 400$ [9]. Differ from Equation (1), the delay dynamic can be described by a delay differential equation:

$$\dot{x}(t) = -x(t) + f(x(t-\tau), u(t)) \qquad (5)$$

where $f(x)$ is the nonlinear transform to the input data, $u(t)$ is the masked input.

The modelling of the hardware implementation is shown in Fig. 2(c). A DRC is formed by a nonlinear circuit with delayed feedback, which is modelled in Simulink. The nonlinear transform is achieved by a bipolar transistor together with voltage divider, which provides a Mackey-Glass typed nonlinear function (Fig. 2(d)) [9]. The settling time is controlled by a low-pass filter. The step response is shown in Fig. 2(e). The pre- and post-processing algorithm of ECG data are done by MATLAB, which will be introduced in next section.

III. Methodology: ECG Signal Processing by DRC

Traditional ECG signal processing for machine learning and classification always involves segmentation, spectrum analyse, feature extraction, QRS detect, interval measurement [13, 14]. However, in order to facilitate the future development of a wearable, pure analogue and ultra-low-power ectopic heartbeat detector device, the ECG signal processing in this paper abandons these procedures which are not desired and achievable for analogue system. Instead, we try to inject the raw ECG data directly to DRC. Here we fully take advantage of the delayed feedback to map a full spectrum of ECG to the reservoir by setting a high ratio of feedback (high β and low γ in Equation (1))

TABLE I
SUMMARY OF SELECTED RECORDS WITH HIGH AMOUNT OF VEB

Record	200	203	208
Gender and age	Male, 64	Male, 43	Female, 23
VEB	**826**	**444**	**992**
Normal	1743	2529	1586
SVEB, F and Q	32	7	377

A. ECG dataset

MIT-BIH Arrhythmia Database contains 48-half-hour ECG data from 47 patients [12]. All the data was sampled at 360Hz by two leads and annotated by at least two cardiologists. According to the recommendations of the Association for the Advancement of Medical Instrumentation (AAMI), the ECG can be arbitrarily classified as five classes: normal, ventricular (VEB), supraventricular (SVEB), fusion of normal and ventricular (F) and unknown beats (Q) [19]. In this paper, the motivation is to detect VEB, an arrhythmia related to various heart diseases such as coronary heart disease and cardiomyopathy, among the dataset. We choose three records with the most VEB (Table I) to test our DRC modelling and only lead MILII was used.

B. Data pre-processing

- Training data and label: training data was randomly collected from the three records. The label was obtained from the annotation of database. All the locations of VEBs are right shifted by 60 points and labelled as 1 while the rest are 0. The reason is that we treat the output also as a time-dependent signal and a peak at the output is expected after a VEB is injected. A piece of training data and labels are shown in Fig. 3(a).
- Signal resampling: the original sampling rate from the database is 360Hz. However, this number creates

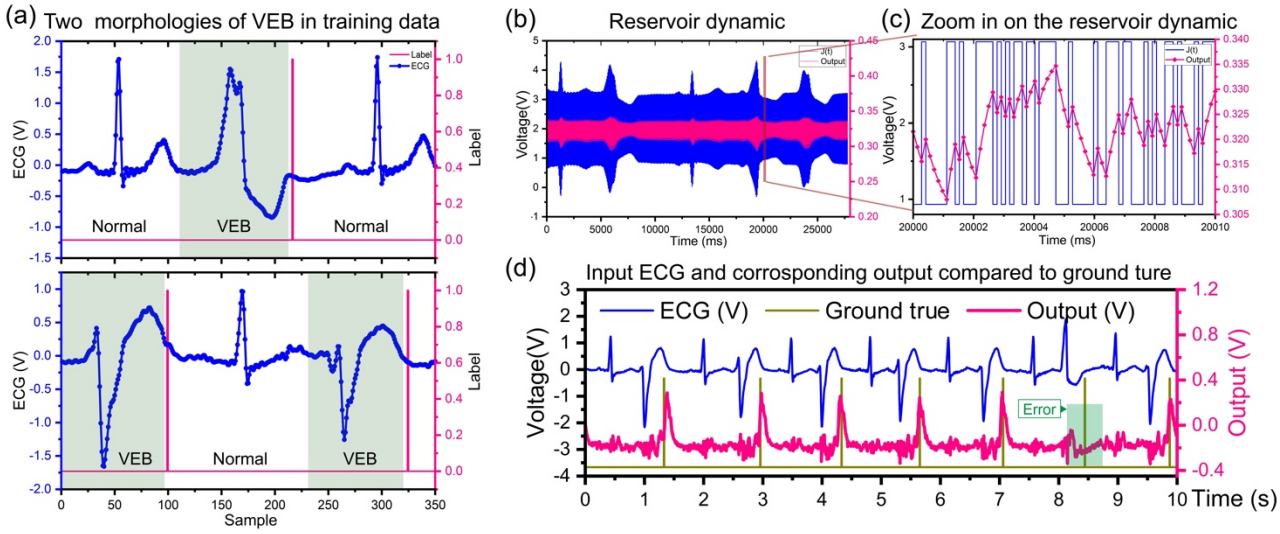

Fig. 3. (a) Two sections of data from the database where the two morphologies of VEB were found. The red line is the annotated location of VEB shifted by 60 samples. (b) and (c) The DRC's input and output. The output presents a dependency of previous output because of the T = 5×θ. (d) An example of raw ECG data, system output and ground truth (expected output). The system responses to most of the VEB except one error which has been highlighted, whereas other types of ECG return minor output. Data illustrated in (b), (c) and (d) are yielded by s = 2 and b = 2 in Equation (6).

redundant samples for detection. Therefore, we resampled the data by 180Hz sampling rate.

- Filtering and normalization: a bandpass range of 0.5-35Hz filter was applied to the data to remove unwanted artefacts and drifts, followed by the data is normalized to 0-1 [13].
- Masking: masking procedure plays an important role to map data to high dimension, which is inspired by the complex dynamic of reservoir computing [8]. With the length of *N*, the mask (M), is a matrix containing randomly allocated -1 and 1. Each data point of ECG (*u(n)*) will be extended to the length of the virtual node (N) by multiplying M:

$$J(k) = u(\lfloor k/N \rfloor) \cdot M(k \bmod N)/s + b \qquad (6)$$

where J(k) denotes the input of the reservoir after pre-processing, s and b are the scale and bias of the input for ensuring the range of *J(k)* is within the effective range of the nonlinear node. The blue line of Fig. 3(b) illustrates the masked signal *J(k)*.

C. Dynamic of hardware-based reservoir

By sampling and holding *J(k)*, we get *J(t)* to be generated and sent to the DRC modelling as shown in Fig. 2(c). Fig. 3(b) also present an example of the input (blue) and output (pink) of the model. As mentioned in Section II, the small θ *(T/5)* results in a more complex dynamic in the reservoir as shown in Fig. 3(c). The current state is related to previous states, which links the neighbouring virtual nodes for a similar complex dynamic of a normal reservoir.

D. Post-processing

A sampling rate of θ is applied to the output and we yield $X_{test}(k)$, followed by the $X_{test}(k)$ is grouped by each N samples for $X_{test}(n) \in \mathbb{R}^{l \times N}$. Using Equation (3) and trained W_{res}^{out}, the reservoir output can be calculated. Fig. 3(d) compares the calculated output and the ground truth from the annotation file. We can observe a clear peak after each VEB occurs.

A peak finder algorithm is used to find the location of VEB among the output *y(n)*. Another algorithm is used to judge the correctness of each location because the result of peak finder cannot be exactly the same as the ground truth. If a peak in ground truth is found near the result, this peak is a correct result.

TABLE II
DETECTION RESULT OF THE THREE RECORDS USING DRC

Record	200	203	208	Avg.
Se (%)	87.87	81.99	92.66	**87.51**
+P (%)	100.00	92.76	97.88	**96.88**
Sp (%)	100.00	97.70	97.14	**98.28**
Acc (%)	94.32	93.54	94.51	**94.12**

IV. Results and Discussion

The DRC is trained by the randomly chosen data as mentioned above. The evaluation was carried out on the entire dataset of Record 200, 203, 208. Their ECG data is processed by the DRC model and a section of the data and output are shown on the top of Fig. 4. After post-processing, the final result is compared with the ground truth (manual diagnosis by at least two cardiologists) from database. According to the AAMI's recommendation, a correctly detected heartbeat is True Positive (*TP*); a missed heartbeat is False Negative (*FN*); an incorrectly detected heartbeat is False Positive (*FP*); a correctly rejected heartbeat is True Negative (*TN*). Using these results, there are four stander statistics that are of interest: sensitivity (*Se*), positive predictive (*+P*), specificity (*Sp*), and accuracy (*Acc*) [19]. Based on this evaluation, the experimental result is illustrated in Fig. 4 and listed in Table II. The hardware-based DRC model yields 87.51% Se, 96.88% +P, 98.28% Sp and 94.12% Acc.

V. Conclusion

In this paper, we introduce a modelling of hardware-based DRC. This model is evaluated by an arrhythmia detection task. Compared with the state-of-the-art software-based approaches, the result is acceptable and, more importantly, it is a hardware-based model as the main information processing unit are analogue electronics with the other blocks also achievable by hardware. This model presents great potential to be the core of the next-generation low-power neuromorphic device for wearable applications, such as wearable low-power long-term arrhythmia detector. Future development will involve pre- and post-processing circuit design, hardware experimentation, plus other types of arrhythmia detection *in vivo*.

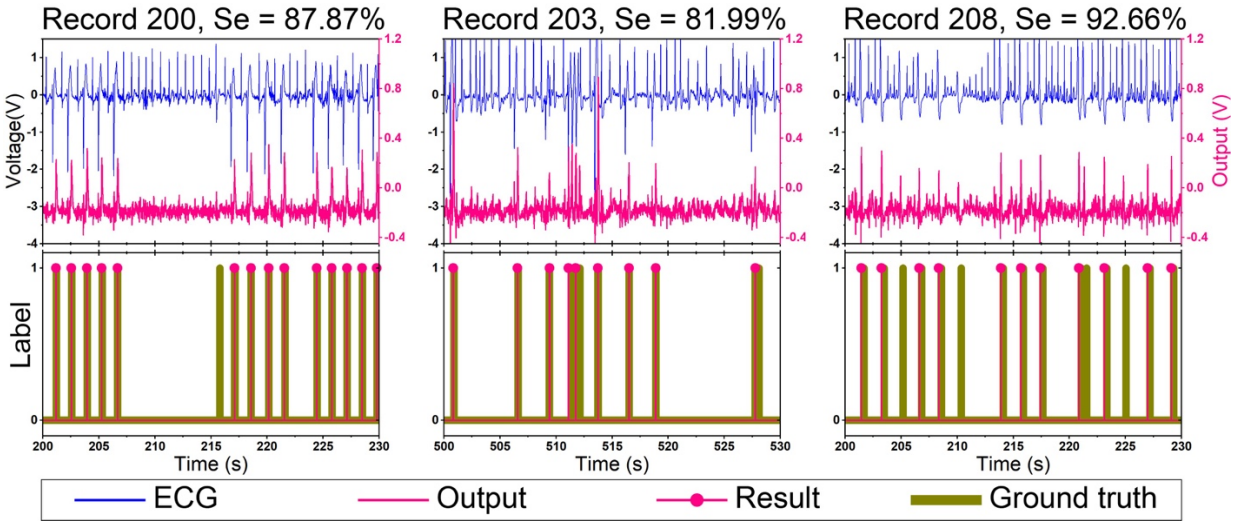

Fig. 4. Results of the three records with high amount of VEB are partially displayed. (Top) The input ECG and output voltage. (Bottom) The comparisons between final result (pink) and ground truth from the annotation files.

REFERENCES

[1] I. Schuller and R. Stevens, "Neuromorphic computing: from materials to systems architecture," *Round Table Report,* 2015.

[2] J. Grollier, D. Querlioz, and M. D. Stiles, "Spintronic Nanodevices for Bioinspired Computing," *Proceedings of the IEEE,* vol. 104, no. 10, pp. 2024-2039, 2016.

[3] C. D. Schuman *et al.*, "A survey of neuromorphic computing and neural networks in hardware," *arXiv preprint arXiv:1705.06963,* 2017.

[4] G. Tanaka *et al.*, "Recent advances in physical reservoir computing: A review," *Neural Networks,* vol. 115, pp. 100-123, 2019/07/01/ 2019.

[5] G. Indiveri and S. Liu, "Memory and Information Processing in Neuromorphic Systems," *Proceedings of the IEEE,* vol. 103, no. 8, pp. 1379-1397, 2015.

[6] X. Liang *et al.*, "Fusion of Wearable and Contactless Sensors for Intelligent Gesture Recognition," *Advanced Intelligent Systems,* vol. n/a, no. n/a, p. 1900088.

[7] X. Liang, R. Ghannam, and H. Heidari, "Wrist-Worn Gesture Sensing With Wearable Intelligence," *IEEE Sensors Journal,* vol. 19, no. 3, pp. 1082-1090, 2019.

[8] L. Appeltant *et al.*, "Information processing using a single dynamical node as complex system," *Nature Communications,* vol. 2, no. 1, p. 468, 2011/09/13 2011.

[9] M. C. Soriano *et al.*, "Delay-Based Reservoir Computing: Noise Effects in a Combined Analog and Digital Implementation," *IEEE Transactions on Neural Networks and Learning Systems,* vol. 26, no. 2, pp. 388-393, 2015.

[10] Y. Paquot *et al.*, "Optoelectronic Reservoir Computing," *Scientific Reports,* Article vol. 2, p. 287, 02/27/online 2012.

[11] J. Torrejon *et al.*, "Neuromorphic computing with nanoscale spintronic oscillators," *Nature,* vol. 547, p. 428, 07/26/online 2017.

[12] G. B. Moody and R. G. Mark, "The impact of the MIT-BIH Arrhythmia Database," *IEEE Engineering in Medicine and Biology Magazine,* vol. 20, no. 3, pp. 45-50, 2001.

[13] S. Ortín, M. C. Soriano, M. Alfaras, and C. R. Mirasso, "Automated real-time method for ventricular heartbeat classification," *Computer Methods and Programs in Biomedicine,* vol. 169, pp. 1-8, 2019/02/01/ 2019.

[14] M. Alfaras, M. C. Soriano, and S. Ortín, "A Fast Machine Learning Model for ECG-Based Heartbeat Classification and Arrhythmia Detection," (in English), *Frontiers in Physics,* Original Research vol. 7, no. 103, 2019-July-18 2019.

[15] M. A. Escalona-Morán, M. C. Soriano, I. Fischer, and C. R. Mirasso, "Electrocardiogram Classification Using Reservoir Computing With Logistic Regression," *IEEE Journal of Biomedical and Health Informatics,* vol. 19, no. 3, pp. 892-898, 2015.

[16] H. Jaeger, "The “echo state” approach to analysing and training recurrent neural networks-with an erratum note," *Bonn, Germany: German National Research Center for Information Technology GMD Technical Report,* vol. 148, no. 34, p. 13, 2001.

[17] W. Maass, T. Natschläger, and H. Markram, "Real-Time Computing Without Stable States: A New Framework for Neural Computation Based on Perturbations," *Neural Computation,* vol. 14, no. 11, pp. 2531-2560, 2002.

[18] W. Wang, X. Liang, M. Assaad, and H. Heidari, "Wearable Wristworn Gesture Recognition Using Echo State Network," in *26th IEEE International Conference on Electronics Circuits and Systems (ICECS)*, 2019.

[19] ANSI/AAMI, "Testing and reporting performance results of cardiac rhythm and ST segment measurement algorithms," *ANSI/AAMI EC38,* vol. 1998, 1998.